# DYNAMIC ANALYSIS OF SPACE SHUTTLE/RMS CONFIGURATION USING CONTINUUM APPROACH

**Jayant Ramakrishnan**
**Dynacs Engineering Company, Inc.**
**Palm Harbor, Florida**

p. 25

**and**

**Lawrence W. Taylor, Jr.**
**NASA Langley Research Center**
**Hampton, Virginia**

## ABSTRACT

The initial assembly of Space Station Freedom involves the Space Shuttle, its Remote Manipulation System (RMS) and the evolving Space Station Freedom. The dynamics of this coupled system involves both the structural and the control system dynamics of each of these components. The modeling and analysis of such an assembly is made even more formidable by kinematic and joint nonlinearities.

The current practice of modeling such flexible structures is to use finite element modeling in which the mass and interior dynamics is ignored between thousands of nodes, for each major component. The model characteristics of only tens of modes are kept out of thousands which are calculated. The components are then connected by approximating the boundary conditions and inserting the control system dynamics.

In this paper continuum models are used instead of finite element models because of the improved accuracy, reduced number of model parameters, the avoidance of model order reduction, and the ability to represent the structural and control system dynamics in the same system of equations. Dynamic analysis of linear versions of the model is performed and compared with finite element model results. Additionally, the transfer matrix to continuum modeling is presented.

The continuum modeling approach is seen to offer a viable alternative to finite element modeling. The continuum approach enables increased insight for synthesis and integrated control/structures design.

## NOMENCLATURE

Symbols

| | |
|---|---|
| A, B, C, D | state vector elements, coefficients of the sinusoidal and hyperbolic functions |
| c | model parameter vector |
| EA | longitudinal stiffness |
| $EI_x$, $EI_y$ | bending stiffness |
| Fo | constant axial force |
| GA | lateral shear |
| GIy | torsional stiffness |
| F | force distribution function |
| $F_o$ | axial, steady force |
| I | inertia matrix |
| L | length of beam |
| $Q_u$ | deflection coefficient matrix |
| $Q_s$ | angular deflection matrix |
| s | real part of the roots |
| Q | state vector, coefficients of sinusoidal and hyperbolic mode shape basis functions |
| s | real part of root |
| w | modal frequency, imaginary part of the roots |
| $\Omega$ | angular velocity vector |

Superscripts

| | |
|---|---|
| T | transpose |
| -1 | inverse |
| • | differention with respect to *t* |
| / | differention with respect to *z* |

Subscripts

| | |
|---|---|
| i | mode index |
| c.g. | center of gravity |
| n | general index |
| x | $x$ axis |
| y | $y$ axis |
| z | $z$ axis |
| y | torsional axis, $z$ |

## INTRODUCTION

The initial assembly of Space Station Freedom involves the Space Shuttle, its Remote Manipulation System (RMS) and the evolving Space Station Freedom. The assembly of the Space Station Freedom is performed by positioning and connecting 22 modules using a remote manipulation system (RMS). The dynamics of this coupled system involves both the structural and the control system dynamics of each of these components. The numerous configurations that result from this assembly process necessitate an efficient procedure for accurately modeling the structural and control dynamics. The modeling and analysis of such an assembly is made even more formidable by kinematic and joint nonlinearities.

Modeling of complex flexible spacecraft is an issue which has far reaching consequences in controller design and the subsequent spacecraft performance. Numerous difficulties in controlling flexible spacecraft have been attributed to inaccuracies in modeling [1]. With higher controller bandwidth, modeling issues assume greater significance. Increased size and more demanding control specifications promise to make high performance control more difficult [2]. Current modeling schemes for the design and analysis of structural and control systems have several limitations [3]. The conventional approach is to use elements which are void of dynamics on the interior of their boundaries. The computational cost and numerical inaccuracies involved in generating solutions to these equations impose a practical limit to the size (and consequently the accuracy) of these structural dynamics models. For problems with minimal control-structure interaction, the finite element models are adequate. High performance control systems will however require increased fidelity and accuracy in the models.

Distributed parameter modeling is proposed in this work to synthesize high fidelity spacecraft models. The distributed parameter models provide a single set of equations for control and structural dynamics. The conventional finite dimensional representation of complex spacecraft by the finite element method suffers from the following drawback. Finite element models are generally too large for control work. One performs model reduction to reduce the model order to controller synthesis amendable dimensions. Spill-over of control energy into the unmodeled modes can result in instability. The proposed approach represents flexible structural members by partial differential equations offering significant advantages in modeling, parameter estimation and the integrated design of control/structural systems [4], [5], [6]. The present method differs from the finite element method in that an individual element can represent all the modes of that "super" element and produce the force and moment vectors at its boundaries. These elements are then connected at their boundaries to form the model of the complete structure. Bishop [7] and Snowdon [8] have studied applications in which a limited number of such elements have been connected to form simple frames. The homogenization technique [9] and [10] for repetitive lattice trusses is particularly useful. For spacecraft control applications, it is necessary to connect many distributed parameter elements to represent the structural dynamics of complex flexible spacecraft. The software programs available for continuum modeling include: Poeleart's [11] DISTEL, Taylor's [12], PDEMOD and Anderson's [13] BUNVIS program. In this work, PDEMOD is used to generate some of the results.

This paper will discuss the generation of the system of partial differential equations for modeling complex, flexible spacecraft. A continuum model of the assembly configurations of the Space Shuttle RMS - Payload will be used to study the control problems involved. Continuum models are shown to have distinct advantages for control applications.

This paper is organized in the following manner. The formulation of the structural dynamics models, the transfer matrix approach to modeling and the control system embedding methods are presented in the next section. The numerical results for a simple model of the Shuttle/RMS Payload assembly are presented. The results compare the modal characteristics obtained using NASTRAN with the continuum results. The concluding remarks identify the salient features of the proposed approach and related modeling and analysis accomplishments to date.

## Discussion

The formulation of the dynamics using a set of distributed parameter elements connected at their boundaries is key to obtaining the objectives of optimal parameter estimation. The types of elements to be considered are (1) rigid body with a full inertia matrix, and (2) dynamic, flexible beam element. The equations of motion for each of these elements will be considered in turn.

## Equations of Motion

A Newtonian or inertial frame of reference is used for the motion of all beam elements and rigid bodies. For example, the point of attachment in the Newtonian axis of a reference, undeflected beam is:

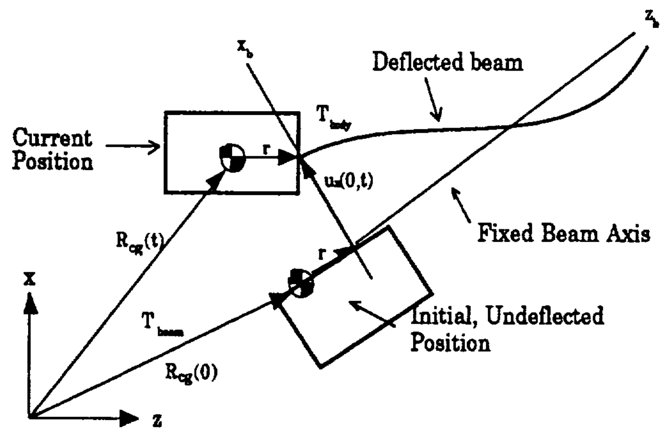


**Figure 1: Diagram of a Rigid Body Attached to its Reference Flexible Beam**

$$R_{\text{attach,o}} = R_{\text{c.g.},o} + T_{\text{beam}} r \tag{1}$$

For the deflected beam:

$$\begin{aligned} R_{\text{attach},t} &= R_{\text{attach}.0} + T_{\text{beam}} u \\ &= R_{\text{c.g.},0} + T_{\text{beam}} r + T_{\text{beam}} u \end{aligned} \tag{2}$$

The position of the body center-of-gravity due to beam deflection is:

$$\begin{aligned} R_{\text{c.g.},t} &= R_{\text{attach},t} - T_{\text{body}} r \\ &= R_{\text{c.g.},0} + T_{\text{beam}} r + T_{\text{beam}} u - T_{\text{body}} r \end{aligned} \tag{3}$$

For small angular deflections

$$T_{\text{body}} = T_{\text{beam}} + \text{Tilda}(T_{\text{beam}} u') \tag{4}$$

Substituting, we get

$$
\begin{aligned}
R_{\text{c.g.},t} &= R_{\text{c.g.},0} + T_{\text{beam}} u - \text{Tilda}\left(T_{\text{beam}} u'\right) r \\
&= R_{\text{c.g.},0} + T_{\text{beam}} u + R\left(T_{\text{beam}} u'\right)
\end{aligned} \tag{5}
$$

Differentiating, we get the acceleration of the body center-of-gravity:

$$
\ddot{R}_{\text{c.g.},t} = T_{\text{beam}} \ddot{u} + \ddot{R}\left(T_{\text{beam}} \ddot{u}'\right) \tag{6}
$$

Equations of motion are written for each rigid body and the forces and moments imparted by the beams are taken into account. In each case it is necessary to account for the different frames of reference and joints of attachment. Equations of motion for the linear and angular degrees of freedom for all of the bodies are assembled into a single matrix, A.

In the time domain the equations of motion are:

$$
\begin{aligned}
\ddot{R}_{\text{c.g}} &= \sum \{\text{Forces}\} / m \\
\dot{\Omega} &= I_{\text{body}}{}^{-I} \sum \{\text{Moments}\}
\end{aligned} \tag{7}
$$

In the frequency domain, the linear and angular equations of motion are the basis for each block of elements:

$$
\begin{aligned}
A_{\text{Linear},j} &= Q_{uj} + T_j^T R_j T_j Q_{uj} - \left(\frac{1}{m_j \omega^2}\right) \sum \left\{ T_j^T T_i P_{Fi} \right\} \\
A_{\text{angular},j} &= Q'_{uj} + T_j^T I_j^{-1} \left(\frac{1}{\omega^2}\right) \sum \left\{ T_{\text{beam-}i} P_{Mi} + R_{\text{beam-}i} T_{\text{beam-}i} P_{Fi} \right\}
\end{aligned} \tag{8}
$$

For each case in which a rigid body has more than one beam attached, a constraint equation is added to the system of equations. Assembly of the equations of motion and the constraint equations yields the system matrix from which we get the characteristic equation:

$$
|A(\sigma + jw)| = 0 \tag{9}
$$

## Flexible Beam Equations

The flexible beam elements exhibit lateral bending in two axes, axial deformation, and torsion. The governing partial differential equations have a variety of terms so that parameter values can select, for example, a wave or string equation, Euler beam equation, or Timoshenko beam equation. A flexible beam element will be described by at least four partial differential equations.

### Lateral Bending

The beam equations represent (1) Euler bending stiffness, (2) axial force stiffness, and (3) Torsion. For bending in the $x$-$z$ plane:

$$Mu_{x,1,tt} + EI_{x,1}u_{x,1,zzzz} + GAu_{x,1,zztt} + F_o u_{x,1,zz} + K_x\left(u_{x,1} + u_{x,2}\right) = F_{x,1}(z,t)$$

$$F_{x,1}(z,t) \qquad (10)$$

### Axial Deformation

Axial dynamics is represented by a wave equation with an additional term which represents a spring connected to a second distributed mass.

$$m\ddot{u}_{z,1} - EAu_{zz,1} + K_z\left(u_{z,2} + u_{z,1}\right) = F_{z,1}(z,t) \qquad (11)$$

### Torsion

Torsional dynamics is represented by a wave equation

$$I_{\psi,1}\ddot{u}_{\psi,1} - GI_{\psi,1}u_{\psi zz,1} + K_\psi\left(u_{\psi,2} + u_{\psi,1}\right) = M_{z,1}(z,t) \qquad (12)$$

### Solution of the Partial Differential Equations

The solutions of these partial differential equations for zero damping produce the sinusoidal and hyperbolic spatial equations which comprise the mode shape functions. For the case that $F_o = 0$, the bending mode shape in the $x$-$z$ plane is:

$$u_x(z) = A_x \sin\beta_{1x}z + B_x \cos\beta_{1x}z + C_x \sinh\beta_{1x}z + D_x \cosh\beta_{1x}z \tag{13}$$

Similarly, for bending in the $y$-$z$ plane:

$$u_y(z) = A_y \sin\beta_{1y}z + B_y \cos\beta_{1y}z + C_y \sinh\beta_{1y}z + D_y \cosh\beta_{1y}z \tag{14}$$

The undamped mode shape functions for torsion and elongation about the $z$ axis are:

$$u_z(z) = A_z \sin\beta_z z + B_z \cos\beta_z z \tag{15}$$

$$u_\psi(z) = A_\psi \sin\beta_\psi z + B_\psi \cos\beta_\psi z \tag{16}$$

These undamped mode shapes are expected to be good approximations to the exact solutions for low level of damping. The mode shape of the entire configuration consists of these functions, repeated for each beam element. Because bending in two directions, torsion and elongation are considered, a total of 12 coefficients are needed. The vector of coefficients is the state vector of the structural dynamics. A vector of the coefficients of these sinusoidal and hyperbolic functions will serve as the state vector.

$$\Theta^T = \left[A_x\ B_x\ C_x\ D_x\ A_y\ B_y\ C_y\ D_y\ A_z\ B_z\ A_\psi\ B_\psi\right] \tag{17}$$

Under conditions of applied forces it is necessary to include rigid body modes. Their coefficients will expand the state vector accordingly. All deflections, forces, moments, and accelerations will be expressed in terms of such state vectors.

The motion of each rigid body is put in terms of the deflection at the point of attachment of a particular reference beam element. The linear and angular deflection vectors can be expressed as:

$$u = Q_u(z)\Theta \tag{18}$$

$$u = Q_s(z)\Theta \tag{19}$$

Next, it is necessary to express the forces and moments at either end of the beam elements. The force and moment vectors are:

$$F_{\text{attach}} = P_F(z)\Theta \tag{20}$$
$$F_{\text{attach}} = P_M(z)\Theta \tag{21}$$

It is also necessary to account for changes in axes from each beam to the body to which it is attached, and for points of attachment at some distance away from the center of gravity. The force and moment that a beam-i applies to a body-j are:

$$F_{\text{body}-j} = T_{\text{body}-j}{}^T T_{\text{beam-}i} P_{F,i}(z)\Theta \tag{22}$$
$$M_{\text{body}-j} = T_{\text{body}-j}{}^T \left\{ T_{\text{beam-}i} P_{M,i}(z) + R_{\text{beam-}i}(z) T_{\text{beam-}i} P_F(z) \right\}\Theta \tag{23}$$

The partial differential equations provide the relationships between the modal frequency and the eigenvalues for the mode shape equations. The lateral beam, axial deformation and torsion equations can be solved for the zero damping cases to produce the following relationships between the modal frequency and the wave numbers in the mode shape function.

For bending in the $x$-$z$ plane:

$$\beta_{1,x^2} = .5b + \sqrt{(.5b)^2 + m\omega^2 / EI_x} \tag{24}$$
$$\beta_{2,x^2} = -.5b + \sqrt{(.5b)^2 + m\omega^2 / EI_x} \tag{25}$$

where $b = m\omega^2 / GA + F_o / EI_x$.

The case for bending in the y-z plane is similar. For torsion and elongation:

$$\beta_\psi = \omega / \sqrt{GI_\psi / m} \tag{26}$$
$$\beta_z = \omega / \sqrt{EA / m} \tag{27}$$

## Transfer Matrix Approach

The transfer matrix approach [14] is suitable for large systems made up of several subsystems. The typical subsystem may be simple elements like a scalar spring or a complex Bernoulli-Euler or Timoshenko beam element. The subsystems are cast in the form of a field and a point matrix. The formulation is in terms of the state vector which is a column matrix of displacements and internal forces. The treatment of the transfer matrix derivation for rigid bodies and flexible beams follows the work in [15].

## Rigid Body

The translational and rotational equations of the $j^{th}$ body can be described by the following equations (figure 2).

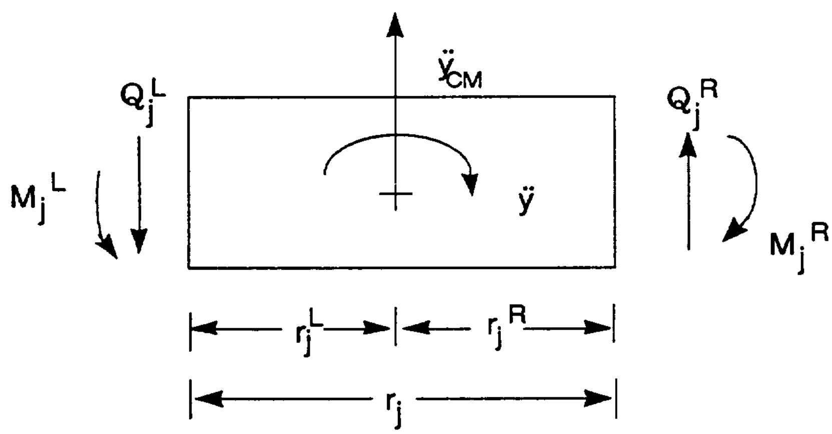


**Figure 2: Free-Body Diagram of the rigid body**

$$m_j\ddot{y}_{CM} = Q_j^R - Q_j^L \tag{28}$$

$$I_j\ddot{y}' = M_j^R - Q_j^R r_j^R - Q_j^L r_j^L \tag{29}$$

For harmonic motion, the equations are rewritten as

$$Q_j^R = Q_j^L - m_j\omega^2 Y_{CM} \tag{30}$$

$$M_j^R = M_j^L + Q_j^R r_j^R + Q_j^L r_j^L - I_j\omega^2 Y_j'^L \tag{31}$$

The displacement of the center of mass $Y_{CM}$ is related to $Y_j^R$ and $Y_j^L$ by

$$Y_j^R = Y_{CM} - r_j^R Y_j'^R \tag{32}$$

$$Y_j^L = Y_{CM} + r_j^R Y_j'^L \tag{33}$$

Using the expression for $Y_{CM}$ from equation (33) and by the property of slope continuity, equation (32) can be rewritten as

$$Y_j^R = Y_j^L - r_j Y_j'^L \tag{34}$$

where $r_j = r_j^L + r_j^R$ .

Substituting for $Y_{CM}$ in equation (30), we get

$$Q_j^R = Q_j^L - m_j \omega^2 \left( Y_j^L - r_j Y_j'^L \right) \tag{35}$$

Substituting the expression for $Q_j^R$ in equation (31), we get

$$M_j^R = M_j^L + r_j Q_j^L - m_j \omega^2 r_j^R Y_j^L - \left( I_j - m_j r_j^L r_j^R \right) \omega^2 Y_j'^L \tag{36}$$

Equations (34), (35), (36) and the slope continuity condition yield the point matrix $[PM]_j$ for the rigid body element

$$[PM]_j = \begin{bmatrix} 1 & -r_j & 0 & 0 \\ 0 & 1 & 0 & 0 \\ -m_j \omega^2 & m_j \omega^2 r_j^L & 1 & 0 \\ m_j \omega^2 r_j^R & -\left( I_j - m_j r_j^L r_j^R \right) & r_j & 1 \end{bmatrix} \tag{37}$$

$$\begin{bmatrix} Y \\ Y' \\ Q \\ M \end{bmatrix}_j^R = [PM]_j \begin{bmatrix} Y \\ Y' \\ Q \\ M \end{bmatrix}_j^L \tag{38}$$

## Flexible Beam

The field matrix for Bernoulli-Euler beam is derived from the solution of the bending mode slope (Equation 13) as follows.

At the left end of the beam ($z = 0$), the displacement $Y(0)$ slope $Y'(0)$, shear force $Q(0)$ and bending moment $M(0)$ will be

$$\begin{bmatrix} Y \\ Y' \\ Q \\ M \end{bmatrix}_{j-1}^{R} = \begin{bmatrix} 0 & 1 & 0 & 1 \\ \beta & 0 & \beta & 0 \\ -k\beta^3 & 0 & +k\beta^3 & 0 \\ 0 & -k\beta^2 & 0 & -k\beta^2 \end{bmatrix} \begin{bmatrix} A_x \\ B_x \\ C_x \\ D_x \end{bmatrix} \tag{39}$$

where $Q = kY'''$ and $M = kY'', k = EI$. For notational simplicity, the subscript $x$ on $\beta$ is dropped. At the right end of the beam ($z = L$)

$$\begin{bmatrix} Y \\ Y' \\ Q \\ M \end{bmatrix}_{j}^{L} = \begin{bmatrix} \sin\beta L & \cos\beta L & \sinh\beta L & \cosh\beta L \\ \beta\cos\beta L & -\beta\sin\beta L & \beta\cosh\beta L & \beta\sinh\beta L \\ k\beta^3\cos\beta L & -k\beta^3\sin\beta L & k\beta^3\cosh\beta L & -k\beta^3\sinh\beta L \\ k\beta^2\sin\beta L & k\beta^2\cos\beta L & -k\beta^2\sinh\beta L & k\beta^2\cosh\beta L \end{bmatrix} \begin{bmatrix} A_x \\ B_x \\ C_x \\ D_x \end{bmatrix} \tag{40}$$

Solving for the coefficients $A_x, B_x, C_x, D_x$ from equation (39) and substituting in equation (40) we get the field matrix for the beam element as:

$$[FM]_j = \begin{bmatrix} \frac{1}{2}(\cos\beta L + \cosh\beta L) & \frac{1}{2\beta}(\sin\beta L + \sinh\beta L) & \frac{1}{2k\beta^3}(\sin\beta L - \sinh\beta L) & \frac{1}{2k\beta^2}(\cos\beta L - \cosh\beta L) \\ \frac{-\beta}{2}(\sin\beta L + \sinh\beta L) & \frac{1}{2}(\cos\beta L + \cosh\beta L) & \frac{1}{2k\beta^3}(\cos\beta L - \cosh\beta L) & \frac{-1}{2k\beta}(\sin\beta L - \sinh\beta L) \\ \frac{-k\beta^3}{2}(\sin\beta L + \sinh\beta L) & \frac{1}{2}k\beta^2(\cos\beta L + \cosh\beta L) & \frac{1}{2}(\cos\beta L - \cosh\beta L) & \frac{-\beta}{2}(\sin\beta L - \sinh\beta L) \\ \frac{k\beta^2}{2}(\cos\beta L + \cosh\beta L) & \frac{1}{2}(\sin\beta L + \sinh\beta L) & \frac{1}{2\beta}(\sin\beta L - \sinh\beta L) & \frac{1}{2}(\cos\beta L - \cosh\beta L) \end{bmatrix}$$

$$\begin{bmatrix} Y \\ Y' \\ Q \\ M \end{bmatrix}_{j}^{L} = [FM]_j \begin{bmatrix} Y \\ Y' \\ Q \\ M \end{bmatrix}_{j-1}^{R} \tag{41}$$

The transfer matrix for a flexible beam with a mass at the right end is

$$[TF]_j = [PM]_j [FM]_j \tag{42}$$

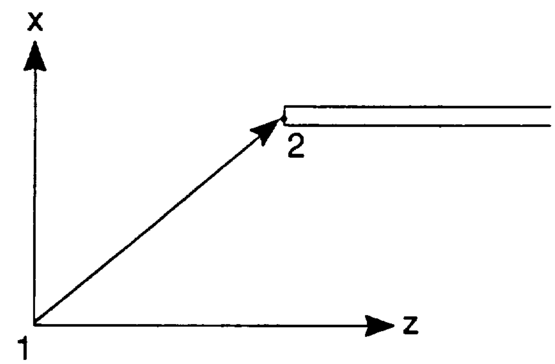


**Figure 3: Beam Offset**

## Offset Attachment

The planar offset attachment transfer matrix can derived from figure 3. The offset of point 2 from the origin (point 1) is given by $r_x$ and $r_z$.

$$\begin{bmatrix} u_x \\ u_z \\ \theta_y \\ F_x \\ F_z \\ M_y \end{bmatrix}_2 = \begin{bmatrix} 1 & 0 & -r_z & 0 & 0 & 0 \\ 0 & 1 & r_x & 0 & 0 & 0 \\ 0 & 0 & 1 & 0 & 0 & 0 \\ 0 & 0 & 0 & 1 & 0 & 0 \\ 0 & 0 & 0 & 0 & 1 & 0 \\ 0 & 0 & 0 & r_z & -r_x & 1 \end{bmatrix} \begin{bmatrix} u_x \\ u_z \\ \theta_y \\ F_x \\ F_z \\ M_y \end{bmatrix}_1 \tag{43}$$

### Joint with Compliance

The joint compliance transfer matrix is derived for planar motion assuming a spring of stiffness $k_\theta$ . The joint equations for planar motion are

$$(M_y)_2 = (M_y)_1 \tag{44}$$

also

$$(M_y)_2 = k_\theta(\theta_1 - \theta_2) \tag{45}$$

The transfer matrix can be expressed as

$$\begin{bmatrix} u_x \\ u_z \\ \theta_y \\ F_x \\ F_z \\ M_y \end{bmatrix}_2 = \begin{bmatrix} 1 & 0 & 0 & 0 & 0 & 0 \\ 0 & 1 & 0 & 0 & 0 & 0 \\ 0 & 0 & 1 & 0 & 0 & -1/k_\theta \\ 0 & 0 & 0 & 1 & 0 & 0 \\ 0 & 0 & 0 & 0 & 1 & 0 \\ 0 & 0 & 0 & 0 & 0 & 1 \end{bmatrix} \begin{pmatrix} u_x \\ u_z \\ \theta_y \\ F_x \\ F_z \\ M_y \end{pmatrix}_1 \tag{46}$$

### Rigid Body Control

The rigid body point matrix for a body with mass and inertia but with $r_j$ equal to zero is obtained from equation (37). Using the Laplace variable $s^2$ in the place of $-\omega^2$ , we get

$$\begin{pmatrix} u_x \\ u_z \\ \theta_y \\ F_x \\ F_z \\ M_y \end{pmatrix}_2 = \begin{bmatrix} 1 & 0 & 0 & 0 & 0 \\ 0 & 1 & 0 & 0 & 0 \\ 0 & 0 & 1 & 0 & 0 \\ Ms^2 & 0 & 0 & 1 & 0 \\ 0 & Ms^2 & 0 & 0 & 0 \\ 0 & 0 & Is^2 & 0 & 1 \end{bmatrix} \begin{pmatrix} u_x \\ u_z \\ \theta_y \\ F_x \\ F_z \\ M_y \end{pmatrix}_1 \tag{47}$$

Rigid body controllers basically stabilize the system asymptotically and are of the proportional derivative type. The transfer matrix is modified in the following manner for control:

$$ms^2 \rightarrow ms^2 + c_x s + k_x$$
$$Is^2 \rightarrow Is^2 + c_\theta s + k_\theta$$

### Joint Control

Analogous to the rigid body controller, it is also possible to embed local feedback control effects into the transfer matrix for a joint. Only one matrix element is affected. For proportional derivative control including sensor $f(s)$ and actuator $g(s)$ dynamics, the matrix in equation (46) is modified thus:

$$1/k_\theta \rightarrow 1/\left[f(s)g(s)(k_1 + k_2 s)\right] \tag{48}$$

### Alignment Matrix

The alignment of each element with respect to global coordinates is accomplished by a simple matrix multiplication. The planar alignment transfer matrix is

$$\begin{bmatrix} u_x \\ u_z \\ \theta_y \\ F_x \\ F_z \\ M_z \end{bmatrix}_2 = \begin{bmatrix} \cos\alpha & -\sin\alpha & 0 & 0 & 0 & 0 \\ \sin\alpha & \cos\alpha & 0 & 0 & 0 & 0 \\ 0 & 0 & 1 & 0 & 0 & 0 \\ 0 & 0 & 0 & \cos\alpha & -\sin\alpha & 0 \\ 0 & 0 & 0 & \sin\alpha & \cos\alpha & 0 \\ 0 & 0 & 0 & 0 & 0 & 1 \end{bmatrix} \begin{bmatrix} u_x \\ u_z \\ \theta_y \\ F_x \\ F_z \\ M_z \end{bmatrix}_1 \tag{49}$$

### End-to-End Transfer Matrix

The transfer matrix which relates the deflections and loads at the space shuttle to those through the RMS to the Space Station consists of the product of all of the elements as shown in Figure 4.

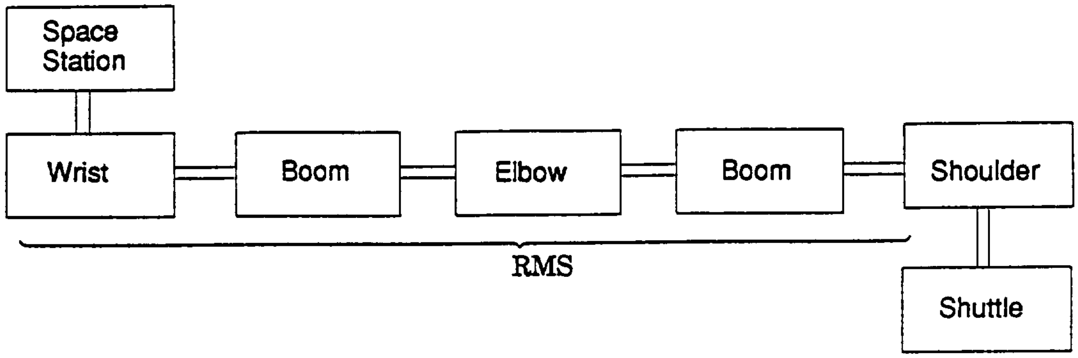


**Figure 4: Shuttle/RMS/Station Configuration**

$$\begin{bmatrix} Y \\ Y' \\ Q \\ M \end{bmatrix}_{\text{station}} = \begin{bmatrix} U_{\text{station}} \; U_{\text{wrist}} \; U_{\text{boom 2}} \; U_{\text{elbow}} \; U_{\text{boom 1}} \; U_{\text{shoulder}} \; U_{\text{shuttle}} \end{bmatrix} \begin{bmatrix} Y \\ Y' \\ Q \\ M \end{bmatrix}_{\text{shuttle}}$$

$$= U_{\text{total}} \begin{bmatrix} Y \\ Y' \\ Q \\ M \end{bmatrix}_{\text{shuttle}} \tag{50}$$

It is now possible to derive the characteristic equation for the total system. The effect of all the control systems will be reflected in the characteristic equation since they form a part of the rigid body and joint transfer matrices.

The transfer matrix forms an intermediate step in the computation of the characteristic equation. For beams and masses connected to one another, the transfer matrix between station 1 and station n is derived by multiplying the appropriate field and point matrices. The expression for a typical problem may be expressed as

$$\begin{bmatrix} Y \\ Y' \\ Q \\ M \end{bmatrix}_n = \begin{bmatrix} \phi_{11} & \phi_{12} & \phi_{13} & \phi_{14} \\ \phi_{21} & \phi_{22} & \phi_{23} & \phi_{24} \\ \phi_{31} & \phi_{32} & \phi_{33} & \phi_{34} \\ \phi_{41} & \phi_{42} & \phi_{43} & \phi_{44} \end{bmatrix} \begin{bmatrix} Y \\ Y' \\ Q \\ M \end{bmatrix}_1 \tag{51}$$

If the boundary is cantilevered, then

$$\begin{bmatrix} Y \\ Y' \\ 0 \\ 0 \end{bmatrix}_n = \Phi \begin{bmatrix} 0 \\ 0 \\ Q \\ M \end{bmatrix}_1 \tag{52}$$

Rearranging the state vector we have

$$[A] \begin{bmatrix} Y_n \\ Y_n^1 \\ Q_1 \\ M_1 \end{bmatrix} = [0] \tag{53}$$

where

$$[A] = \begin{bmatrix} -1 & 0 & \phi_{13} & \phi_{14} \\ 0 & -1 & \phi_{23} & \phi_{24} \\ 0 & 0 & \phi_{33} & \phi_{34} \\ 0 & 0 & \phi_{43} & \phi_{44} \end{bmatrix} \tag{54}$$

The characteristic equation is given by

$$\det[A] = 0 \tag{55}$$

or

$$\det[\Phi_{22}] = 0$$

or

$$\phi_{33}\,\phi_{44} - \phi_{34}\,\phi_{43} = 0 \tag{56}$$

For continuum models, equation (56) has infinite solutions and is solved by search techniques to determine the frequencies. Similar characteristic equations can be derived for other boundary conditions.

For free-free boundary conditions, the characteristic equation is given by

$$\det[\Phi_{21}] = 0$$

The transfer function relating the linear and angular deflection of the shuttle (for example) to applied forces and moments are:

$$\begin{bmatrix} Y \\ Y' \end{bmatrix}_{\text{shuttle}} = \Phi_{21}^{-1}\,\Phi_{22}\begin{bmatrix} F \\ M \end{bmatrix}_{\text{shuttle}}$$

The Shuttle/RMS/Payload configuration is now studied from the continuum viewpoint.

## Study of Shuttle/RMS/Payload Assembly

The Space Shuttle/RMS/Payload assembly is modeled and analyzed using the continuum and the finite element approach. For the continuum analysis, the planar transfer matrix approach is used to generate the frequencies of the configuration and the transient response of the structure.

The data for the two link RMS configuration is extracted from the payload deployment and retrieval document [16]. Links 3 and 4 of the RMS arm are used in the simulation. In this work, each link was assumed to be made-up of one material with uniform section properties unlike reference [16] where the links were made-up of 3 segments each with different properties. The link properties are listed in Table 1.

The space shuttle and payload are modeled as rigid bodies with a mass of 6176 slugs and 124.22 slugs respectively. The inertia $I_{yy}$ of the space shuttle is 6.99 E6 lbs-in$^2$.

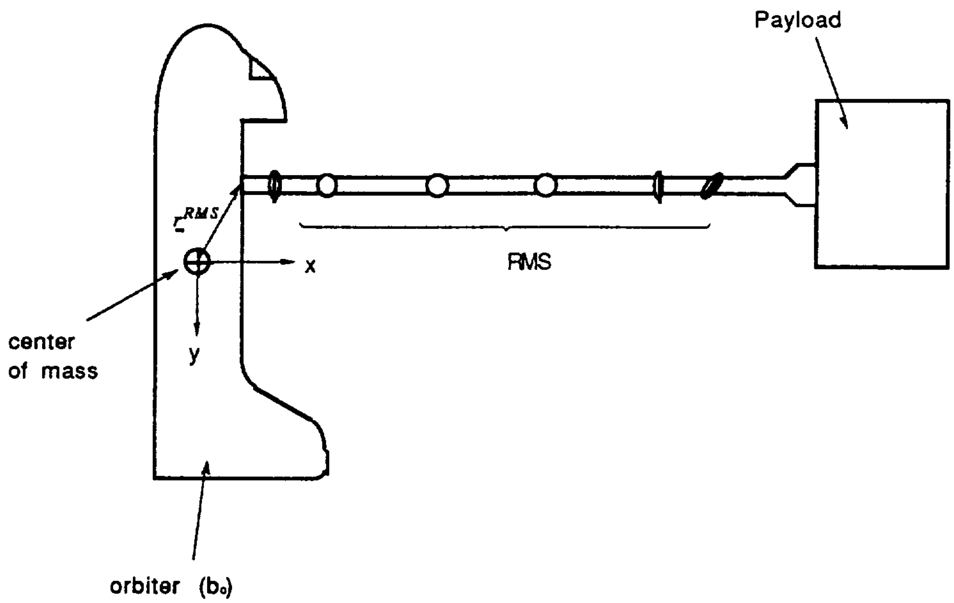


**Figure 5: Shuttle/RMS/Payload Configuration**

Figure 5 shows the Shuttle/RMS/Payload Configuration. The following three cases are considered in this work:

Case 1: Shuttle with zero inertia and offset
Case 2: Shuttle with inertia and zero offset
Case 3: Shuttle with inertia and offset

For the transfer matrix approach, the relationship between the shuttle and the payload is

$$[TM] = \left[U_{\text{payload}}\ U_{\text{link } 2}\ U_{\text{link } 1}\ U_{\text{shuttle}}\right]$$

The characteristic equation for the free-free configuration is derived and the frequencies are evaluated. In order to obtain the $y$-$z$ bending frequencies, the characteristic equation is again solved numerically using the appropriate flexural rigidity value. The results are compared with the frequencies from PDEMOD.

The NASTRAN model of the Shuttle/RMS/Payload assembly consisted of the RMS being modeled using 50 bar elements each. The shuttle and the payload were modeled using two concentrated masses at either end of the RMS. For the shuttle with inertia and offset case, the concentrated mass card in NASTRAN was suitably modified.

**Table 1: RMS Link Properties**

| Property | Link 1 | Link 2 |
|---|---|---|
| mass | 9.5485 slugs | 5.9901 slugs |
| length | 21.0 ft | 23.0 ft |
| EIyy | 5.6458 E6 $lbft^2$ | 3.4166 E6 $lbft^2$ |
| EIzz | 5.2083 E6 $lbft^2$ | 2.4375 E6 $lbft^2$ |
| G | 3.846 E5 psf | 3.846 E5 psf |
| J | 6.7711 $ft^4$ | 5.0558 $ft^4$ |
| m/l | 0.4547 slug/ft | 0.2604 slug/ft |
| A | 0.9218 $ft^2$ | 0.9218 $ft^2$ |

The frequency spectrum in Hertz of the three configurations is shown in Tables 2-4.

**Table 2: Frequencies for Case 1**

| Mode | NASTRAN | PDEMOD | Transfer |
|---|---|---|---|
| 1 | 2.054 | ? | ? |
| 2 | 2.527 | 2.528 | 2.528 |
| 3 | 2.862 | 2.863 | 2.862 |
| 4 | 10.629 | 10.63 | 10.629 |
| 5 | 11.747 | 11.74 | 11.747 |
| 6 | 18.479 | ? | ? |
| 7 | 23.171 | 23.17 | 23.171 |
| 8 | 25.963 | 25.96 | 25.964 |

**Table 3: Frequencies for Case 2**

| Mode | NASTRAN | PDEMOD | Transfer |
|---|---|---|---|
| 1 | 0.1825 | 0.1961 | 0.1892 |
| 2 | 2.0548 | 2.0133 | ? |
| 3 | 2.8627 | ? | ? |
| 4 | 4.2036 | 4.2065 | 4.2033 |
| 5 | ? | 4.6983 | 4.6973 |
| 6 | | 7.6745 | ? |
| 7 | 11.7471 | ? | ? |
| 8 | 13.3324 | 13.3356 | 13.3337 |

**Table 4: Frequencies for Case 3**

| Mode | NASTRAN | Transfer |
|---|---|---|
| 1 | ? | 0.3428 |
| 2 | ? | 0.3685 |
| 3 | 4.2037 | 4.4246 |
| 4 | 4.7001 | 4.9433 |
| 5 | ? | 9.8986 |
| 6 | ? | 9.9017 |
| 7 | 13.3339 | 13.5996 |
| 8 | 14.7421 | 15.0281 |

Figure 6 shows a transient response obtained from PDEMOD for a similar configuration with and without joint control. The results show the promise of the continuum approach.

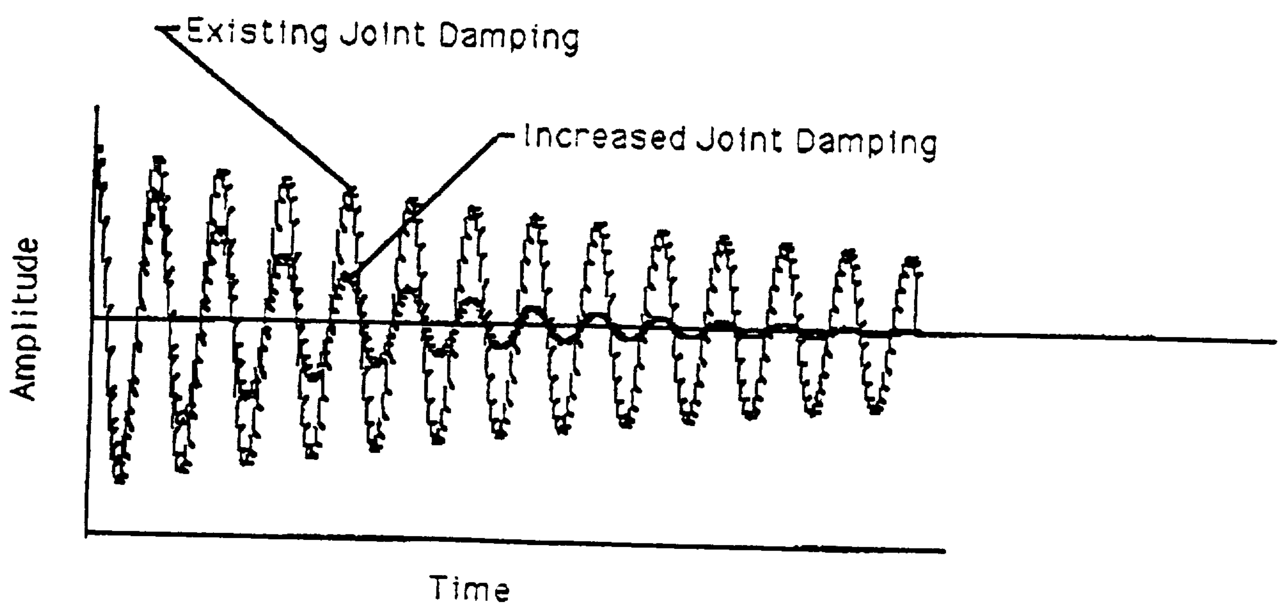


**Figure 6: Transient response of MB-1 Configuration**

## CONCLUDING REMARKS

Partial differential equation models of flexible structures offer significant advantages over finite element models for parameter estimation and control studies because of the smaller number of model parameters. Until recently work was needed to generate distributed parameter models of complex configurations which were also flexible. The computer program, PDEMOD, enables the generation of distributed parameter models of flexible spacecraft. Any configuration which can be modeled by a network of flexible beam elements and rigid bodies can be modeled using PDEMOD. The modeling process is well suited for the evolving Space Station Freedom, for the cases in which (1) the Space Station assembly is attached to the Shuttle, (2) the assembly is linked to the Shuttle through the RMS arm, and (3) the Space Station assembly is free of the Shuttle.

Comparisons of the model accuracy of finite element and continuum models of flexible structures point out the limitations of finite element modeling. First, the level of complexity that is practical for finite element models is limited because of the computational burden. The result is a limit to the accuracy that can be obtained. Second, as high levels of accuracy are sought using finite element models, the difficulties in solving the eigenvalue problem become more significant. It is quite possible, then, that for certain applications continuum models can be more accurate.

A distributed parameter model of the Space Shuttle-RMS was generated using the transfer matrix method and the software PDEMOD. The results show a very good agreement with a detailed finite element model. Future directions include the frequency characterization of structures with embedded control.

### Acknowledgements

The authors wish to thank Mr. Steve Karnyski for his support in simulating different configurations. Ms. Linda Large's help in document preparation is greatly appreciated.

## REFERENCES

1. Likins, Peter W.; and Bouvier, H. Karl (1971), Attitude Control of Nonrigid Spacecraft. Astronautics and Aeronautics.

2. Tolivar, A. F. (1982). NASA LSS Missions and Control Requirements. NASA Workshop on Applications of Distributed System Theory to the Control of LSS, JPL, Pasadena, California, July.

3. Pappa, Richard; Miserentino, Bob; Bailey, Jim; Elliott, Ken; Perez, Cooper, Paul; and Williams, Boyd (1990), Mini-MAST Control Structure Interaction Testbed: A User's Guide, NASA TM - 102630, March.

4. Armstrong, Ernest S. Distributed System Research Motivated by Large Space Structures. IFIP-TC7 Conference on Control Problems for Systems Described by Partial Differential Equations and Applications. Gainesville, Florida, 1986.

5. Taylor, Lawrence W., Jr. and H. Rajiyah (1991), "Applications of Partial Differential Equation Modeling," Spaceflight Mechanics Meeting, Houston, Texas, February 1991.

6. Thomas, Segun (1989, "A Continuum Model for Dynamic Analysis of the Space Station," IAF, International Astronautical Congress, 40th, Malaga, Spain, October 7-13.

7. Bishop, R. E. D. and D. C Johnson, "The Mechanics of Vibration", Cambridge University Press, Cambridge.

8. Snowdon, "Vibration and Shock in Damped Mechanical Systems", John Wiley and Sons, New York.

9. Blankenship, Gilmer L (1988), "Applications of Homogenization Theory to the Control of Flexible Structures", IMA Volume 10, Stochastic Differential Systems, Stochastic Control Theory and Application, Springer-Verlag, New York.

10. Noor, Ahmed K.; Anderson, M. S.; and Greene, W. H. (1978), "Continuum Models for Beam- and Plate-Like Lattice Structures", AIAA Journal, 16, pp. 1219-1228.

11. Poelaert, D. (1983). DISTEL, "A Distributed Element Program for Dynamic Modelling and Response Analysis of Flexible Spacecraft", Dynamics and Control of Large Structures, Fourth VPI&SU/AIAA Symposium, Blacksburg, Virginia.

12. Taylor, Lawrence W., Jr. (1990), "PDEMOD - Computer Software for Partial Differential Equation Modeling of Flexible Spacecraft", 2nd USAF/NASA Workshop on System Identification and Health Monitoring of Precision Space Structures, Pasadena, California.

13. Anderson, Melvin S.; and Williams, F. W. (1987), "BUNVIS - RG: Exact Frame Buckling and Vibration Program, with Repetitive Geometry and Substructuring", Journal of Spacecraft and Rockets, Vol. 24, No. 4, July-August, page 353.

14. Pestel E.C. and Leckie, F.A., "Matrix Methods in Elastomechanics", McGraw Hill Book Company, Inc., New York, 1963.

15. Shen, J.Y. and Taylor, L.W., "Application of the Transfer Matrix Method to Estimate the modal Characteristics of the NASA Mini Mast Truss", NASA Technical Memorandum XXX 1990.

16. NASA Johnson Space Center, "Payload Deployment and Retrieval System Simulation Database, Version 1.0, Flight Support Equipment, RMS Operations", Document No: JSC-25134, July, 1991.

# CONTROL OF FLEXIBLE SYSTEMS

PRECEDING PAGE BLANK NOT FILMED

PAGE 404 INTENTIONALLY BLANK